Zic2 Controls Cerebellar Development in Cooperation with *Zic1*

Jun Aruga,[1] **Takashi Inoue,**[1,2] **Jun Hoshino,**[1,2] **and Katsuhiko Mikoshiba**[1,2]

[1]*Laboratory for Developmental Neurobiology, RIKEN Brain Science Institute, Wako-shi, Saitama 351-0198, Japan, and* [2]*Department of Molecular Neurobiology, Institute of Medical Science, University of Tokyo, Minato-ku, Tokyo 108-8639, Japan*

Mouse *Zic* genes encode zinc finger proteins and are expressed in the developing and mature CNS. Reduced expression of *Zic2* in mice results in spina bifida and holoprosencephaly. However, the disruption of *Zic1*, a strong homolog of *Zic2* that has an overlapping expression pattern, results in cerebellar malformation with no apparent abnormalities in the forebrain or in posterior neuropore closure. Here we revealed that *Zic2* and *Zic1* cooperatively control cerebellar development by regulating neuronal differentiation. Both *Zic1* and *Zic2* are expressed in the precursor cells of the granule neuron and the neurons in cerebellar nuclei. Mice carrying one mutated *Zic1* allele together with one mutated *Zic2* allele ($Zic1^{+/-}Zic2^{+/kd}$) showed a marked cerebellar folial abnormality similar to, but distinct from that found in mice homozygous for the *Zic1* mutation ($Zic1^{-/-}$). The $Zic1^{+/-}Zic2^{+/kd}$ cerebellum is missing a lobule in the anterior vermis and has a truncation of the most posterior lobule. Expression of transverse zonal markers is shifted anteriorly in the developing cerebellum, indicating that the anterior part of the cerebellum is poorly developed. Abnormalities in the developing $Zic1^{+/-}Zic2^{+/kd}$ cerebellum share the following features with those of the $Zic1^{-/-}$ cerebellum: a preceding reduction of cell proliferation in the anterior external germinal layer, a reduction in *cyclin D1* expression, and enhanced expression of the mitosis inhibitors *p27* and *p16*, and enhancement of *Wnt7a* expression. These results indicate that *Zic1* and *Zic2* may have very similar functions in the regulation of cerebellar development.

Key words: Zic1; Zic2; transcription factor; cerebellum; cerebellar foliation; neuronal differentiation

The mammalian cerebellum is composed of multiple folia and fissures that show a uniform and predictable pattern within a given species (Altman and Bayer, 1997; Voogd, 1998). This elaborate pattern of foliation involves the coordinated expression of genes within specific locations in the developing neural tube. Recent studies using genetically modified mice have revealed several genes controlling cerebellar development (Hatten et al., 1997; Herrup and Kuemerle, 1997; Wassef and Joyner, 1997; Goldowitz and Hamre, 1998).

Mouse *Zic1* is one of the genes controlling cerebellar development (Aruga et al., 1994; 1998). *Zic1* is expressed in the dorsal neural tube and its derivatives and is strongly expressed in the developing and mature cerebellum. In the *Zic1*-deficient ($Zic1^{-/-}$) mice, the cerebella are hypoplastic, and their folia are malformed. The abnormalities are closely related to the loss of granule cells, which is most dramatic in the anterior vermis.

Several other *Zic*-related genes have also been identified and implicated in neural development in mice and other species. Among the mouse *Zic* genes, *Zic2* is most similar to *Zic1* (Aruga et al., 1996) and is expressed in overlapping regions (Nagai et al., 1997). However, the phenotypes of the mutant mice with reduced expression of *Zic2* ($Zic2^{kd/kd}$; *kd, knock-down*) are rather different from those of *Zic1*-defient mice. The $Zic2^{kd/kd}$ mice show holoprosencephaly and spina bifida (Nagai et al., 2000), which derive from malformations in the anterior and posterior ends of the neural tube, respectively. The apparent differences in the mutant phenotypes raise the question of whether *Zic1* and *Zic2* are functionally related.

To address this question, we first examined the cerebellar abnormalities in the $Zic2^{kd/kd}$ mice. Because these mice die just after birth with severe brain deformities, we were not able to detect any abnormalities similar to those of *Zic1*-deficient mice. As many vertebrate genes can be functionally compensated by structurally related genes, we started generating mice with *Zic1*/*Zic2* compound mutations. Mice carrying mutations in one allele of *Zic1* and one allele of *Zic2* ($Zic1^{+/-}Zic2^{+/kd}$) showed a behavioral abnormality with cerebellar malformation. This indicates that mouse *Zic2* is involved in cerebellar patterning in cooperation with *Zic1*.

Furthermore, a number of genes controlling cell proliferation and differentiation are deregulated in the cerebella of both $Zic1^{+/-}Zic2^{+/kd}$ and $Zic1^{-/-}$ mice, suggesting that both *Zic1* and *Zic2* function upstream of these genes to regulate cerebellar development.

MATERIALS AND METHODS

Mutant mice. Mice heterozygous for the *Zic1* "null" mutation (Aruga et al., 1998) were backcrossed onto C57BL/6 mice 7–10 times, and mice heterozygous for the *Zic2* "knock-down" mutation (Nagai et al., 2000) were backcrossed four or five times. These backcrossed mice were then used in subsequent matings. Mice were genotyped and maintained as described (Aruga et al., 1998; Nagai et al., 2000). Noon of the day on which vaginal plugs were first observed in the morning was defined as embryonic day 0.5 (E0.5). The mice were maintained by the Advanced Technology Development Center, RIKEN Brain Science Institute and Division of Experimental Animal Research, Tsukuba Life Science Center, RIKEN. All animal experiments were done according to the guidelines for animal experimentation in RIKEN.

Histology and morphometric analysis. For histological examination, tissue was fixed in Bouin's fixative and processed for paraffin sections and

stained with hematoxylin and eosin. The morphometric analysis was performed as described (Aruga et al., 1998). Serial sagittal sections (6 µm) were prepared, and the most comparable sets of sections was selected for the analysis. All the pictures were first digitized by Fuji HC-2500 3CCD camera. The areas were measured using density slice function of NIH Image program (developed at the National Institutes of Health, Bethesda, MD; available on the Internet at http://rsb.info.nih.gov/nih-image/). EGL length was calculated by the same software, measuring manually fitted curves on the EGL. The subjects for the morphometric analysis in this study were two sets of ($Zic1^{+/+}$, $Zic2^{+/+}$), ($Zic1^{+/-}$, $Zic2^{+/+}$), ($Zic1^{+/+}$, $Zic2^{+/kd}$), and ($Zic1^{+/-}$, $Zic2^{+/kd}$) at post-natal day 16 (P16), three pairs of $Zic2^{+/+}$ and $Zic2^{+/kd}$, and two pairs of $Zic2^{+/+}$ and $Zic2^{+/kd}$ at 1 year old. Each set or pair was derived from the same litter.

In situ *hybridization and immunohistochemistry. In situ* hybridization was performed as described (Nagai et al., 1997) with *Zic1, Zic2,* and *En2* probes (Aruga et al., 1994, 1998; Nagai et al., 1997). Cryosections were prepared at 10 µm. Adjacent sections were used in hybridizations to compare the distribution of two different transcripts.

For immunohistochemical staining, cryosections were incubated for 12 hr at 4°C with antibody binding solution consisting of primary antibody [anti-calbindin (Chemicon, Temecula, CA), anti-Eph3 (Santa Cruz Biotechnology, Santa Cruz, CA), anti-βIII tubulin (Promega, Madison, WI), anti-p16 (Santa Cruz Biotechnology), and anti-phospho-histone H3 antibody (Upstate Biotechnology, Lake Placid, NY)], 2% normal goat serum, and 0.1% Triton X-100 in PBS. The bound primary antibody was detected by Cy3-conjugated anti-rabbit IgG, TRITC-conjugated anti-mouse IgG (Jackson ImmunoResearch, West Grove, PA), or a vector stain ABC kit (Vector Laboratories, Burlingame, CA). Immunohistochemical staining with anti-phospho-histone H3 antibody was performed on four pairs of ($Zic1^{+/+}$, $Zic2^{+/+}$) and ($Zic1^{+/-}$, $Zic2^{+/kd}$) embryos. Five comparable sections were prepared from each embryo, and the mean number of the labeled cells were calculated. Statistical significance was determined using a *t* test. *P* values < 0.05 were considered significant.

RT-PCR analysis. E17.5 cerebella from each genotype were excised and frozen in liquid nitrogen. Cerebellar peduncles were trimmed, and pia maters were peeled off before freezing. Total RNA was isolated using Trizol reagent (Life Technologies, Gaithersburg, MD). After DNaseI treatment, reverse transcription was performed with Superscript II reverse transcriptase (Life Technologies). Glyceraldehyde-3-phosphate dehydrogenase (G3PDH) expression was measured to monitor RNA recovery. RT-PCR was performed after they were in the log-linear phase of the amplification curve at the indicated cycles. The PCR cycles, annealing temperature, and primer sequences are: *G3PDH,* 23 cycles, 68°C, 5′ CCGGTGCTGAGTATGTCGTGGAGTCTAC 3′ and 5′ CTTTCCAGAGGGGCCATCCACAGTCTTC 3′; *cyclin D1,* 30 cycles, 55°C, 5′ AACTACCTGGACCGCTTCCT 3′ and 5′ CCACTTGAGCTTGTTCACCA 3′; *cyclin D2,* 26 cycles, 55°C, 5′ AGACCCATCTTCAGCTCCTG 3′ and 5′ TGCTCAATGAAGTCGTGAGG 3′; *p27,* 30 cycles, 55°C, 5′ CTGTGTGCAGTCGCAGAACT 3′ and 5′ CCAGGGGCTTATGATTCTGA 3′; and *Wnt7a,* 32 cycles, 55°C, 5′ CACAGTTCCGAGAGCTAGGC 3′ and 5′ CCTGTCACTGGGTCCTCTTC 3′.

RESULTS

Expression of mouse *Zic2* in the developing cerebellum

We have previously shown the expression pattern of *Zic2* at times earlier than E14 (Nagai et al., 1997). To clarify the role of *Zic2* in cerebellar development, we first examined the expression of *Zic2* at later stages (Fig. 1), compared with that of *Zic1*. Sagittal sections of E16 and E18 brains showed very similar expression patterns for the two genes (Fig. 1*K,L,O,P*), both being strongly expressed in the external germinal layer (EGL) and rhombic lip of the cerebellum and pons in the hindbrain structure. In the telencephalon and mesencephalon, they are expressed in the medial septal nucleus, the thalamic nuclei, and preoptic nucleus.

In coronal sections of the same stage, there was a region expressing *Zic1* and *Zic2* in the midline of the cerebellum that was widest at the ventral part of the cerebellar anlagen (Fig. 1*A–H*). In horizontal sections at E18, *Zic2* expression is composed of three lines, whereas *Zic1* was expressed in a single region

that was strongest in the midline (Fig. 1*J,N*). They are similarly expressed at E16 (Fig. 1*I,M*). The midline expression of *Zic1* and *Zic2* corresponds to a weak but significant expression in the center of the cerebellar primordia in the midsagittal sections (Fig. 1*K,O, asterisk*). Along the anterior–posterior (AP) axis, *Zic1* is more specifically expressed in the midline of the anterior region. In the mature brain, *Zic2* and *Zic1* are expressed in almost identical patterns (Aruga et al., 1998; data not shown).

The cerebellar abnormalities in the $Zic1^{+/-}Zic2^{+/kd}$ mice

We next examined cerebellar phenotypes of the *Zic2* knock-down mice ($Zic2^{kd/kd}$). In the wild-type E16 cerebellum, the left and right cerebellar plates are fusing at the midlines, and one can normally observe a shallow groove at the ventral side of the cerebellar primordia in coronal section (Fig. 2*A*). There was a narrow groove at the midline of the $Zic2^{kd/kd}$ cerebellum (Fig. 2*C*), and the ventricular spaces and the subarachnoid space were markedly reduced. In contrast to these gross morphological abnormalities, there was no obvious histological abnormality (Fig. 2*B,D*). $Zic2^{kd/kd}$ mice had shrinkage or dilatation of the ventricles at the later embryonic stages, which may have been caused by disturbed CSF circulation because of major neural tube anomalies present (spina bifida, holoprosencephaly, and exencephaly) (data not shown).

Because the $Zic2^{kd/kd}$ phenotype was less informative about the role of *Zic2* in cerebellar development, we next asked whether *Zic2* may act in cooperation with *Zic1*. To address this question, we started generating *Zic1*/*Zic2* compound mutant mice. This was possible because *Zic1* and *Zic2* are located on different chromosomes (chromosome 9 and 14, respectively). Initially, we had planned matings between $Zic1^{+/-}Zic2^{+/kd}$ mice to obtain double homozygous mutant mice. However, the $Zic1^{+/-}Zic2^{+/kd}$ mice had a poor survival rate. The frequency of the genotypes obtained by the mating between $Zic1^{+/-}$ and $Zic2^{+/kd}$ mice were: $Zic1^{+/-}Zic2^{+/kd}$, 8%; $Zic1^{+/-}Zic2^{+/+}$, 29%; $Zic1^{+/+}Zic2^{+/kd}$, 29% and $Zic1^{+/+}Zic2^{+/+}$, 34% ($n = 115$) at 4 weeks after birth. In addition, the $Zic1^{+/-}Zic2^{+/kd}$ mice frequently showed hydrocephalus (four of nine at 4 weeks) and always showed a gait and postural abnormalities. We therefore gave up mating between $Zic1^{+/-}Zic2^{+/kd}$ mice and investigated the abnormalities appearing in the $Zic1^{+/-}Zic2^{+/kd}$ mice.

First, the mature brain was examined macroscopically. There was a marked change in the fissure pattern in the cerebellum. The mutant cerebellum apparently lacks the primary fissure in the vermis and posterior superior fissure in the hemisphere (Fig. 3). Comparison of parasagittal sections through the median vermis and the hemisphere indicated that a lobule in the anterior lobe was missing (Fig. 4). Although folial identities are not conclusive at this point, we assigned presumable numbers to the lobules, as in Figures 2, *B* and *C*, and 3*D*. The elongated lobule VI covers the anterior lobe, whereas lobule IX is stubbed in comparison with the wild type. In $Zic1^{+/-}$ mice, lobule V was slightly smaller than the wild type, consistent with a previous study (Aruga et al., 1998), whereas the $Zic2^{+/kd}$ did not show any significant alterations (Fig. 4*C,E*). Foliation patterning in the cerebellar hemisphere was also altered in the $Zic1^{+/-}Zic2^{+/kd}$ mice (Fig. 4*D, right*). In this case, the position of simple lobules shifted anteriorly, and the CrusI of the ansiform lobule extended anteriorly in a similar manner to the change in lobule VI of the vermis.

These features are essentially similar to the folial abnormality in the $Zic1^{-/-}$ cerebellum (Aruga et al., 1998) in that a lobule in
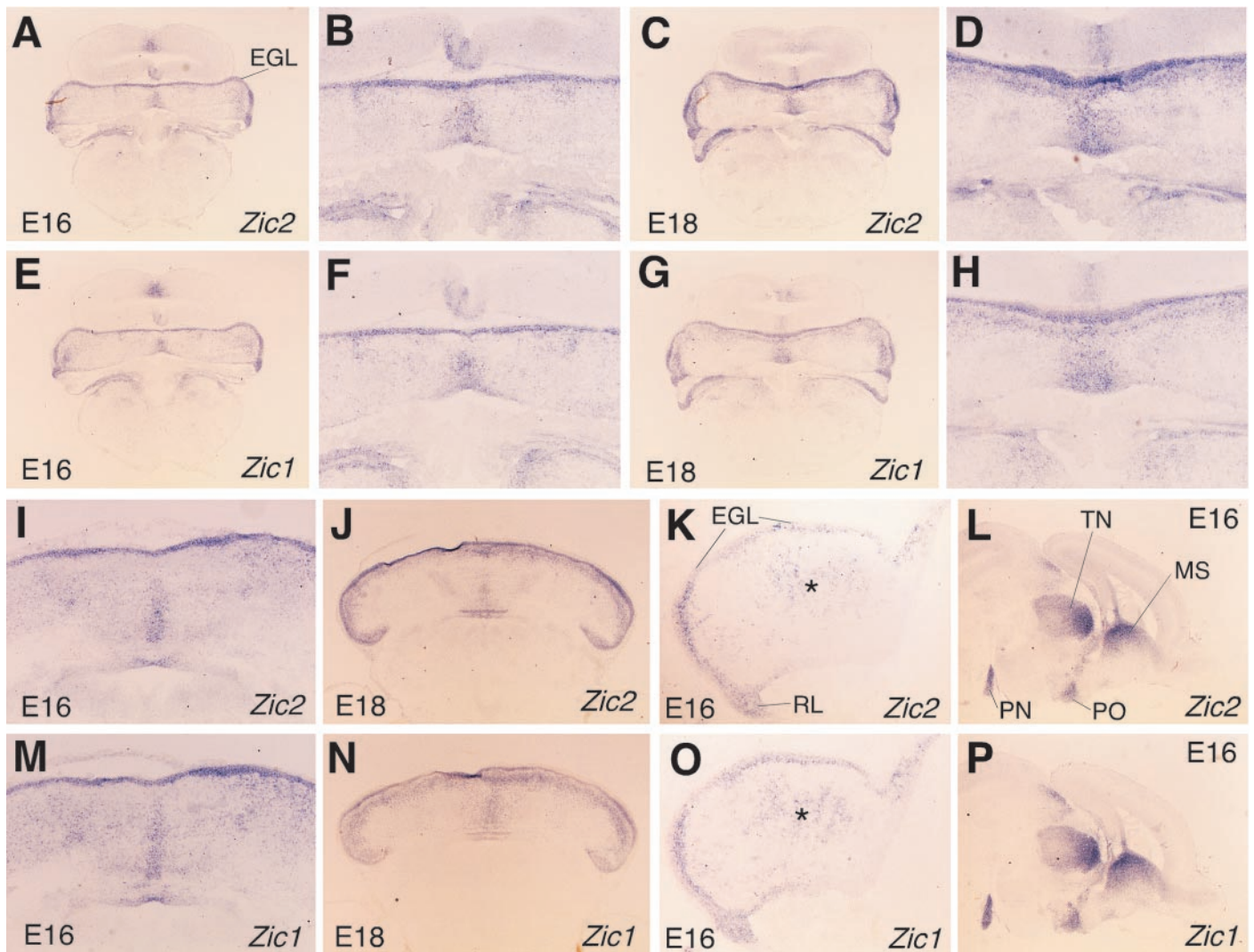
Figure 1. The expression of *Zic1* and *Zic2* in the developing cerebellum. *In situ* hybridization was performed on coronal (*A–H*), horizontal (*I, J, M, N*), and sagittal (*K, L, O, P*) sections of E16 (*A, B, E, F, I, K, L, M, O, P*) and E18 (*C, D, G, H, J, N*) wild-type cerebella with *Zic2* (*A–D, I–L*) and *Zic1* (*E–H, M–P*) probes. *B, D, F,* and *H* are higher magnifications of *A, C, E,* and *G,* respectively. *Zic1* and *Zic2* are expressed in a similar pattern. A significant difference between *Zic1* and *Zic2* expression was found in the vermal (medial) intermediate region (*I, J, M, N*). *Asterisks* in *K* and *O* indicate midsagittal expression in *I* and *M,* respectively. *EGL,* External germinal cell layer; *MS,* medial septum; *PN,* pontine nuclei; *PO,* preoptic nuclei, *TN,* thalamic nuclei.

the anterior lobe is missing. However, there are some differences. First, the cerebellum in the $Zic1^{+/-}Zic2^{+/kd}$ mouse is not as small as that in the $Zic1^{-/-}$ mouse, which shows a greater reduction in the medial to lateral aspect. Second, the extension of lobule VI was greater than that seen in the $Zic1^{-/-}$ cerebellum. Third, the truncation of lobule IX is observed only in $Zic1^{+/-}Zic2^{+/kd}$ cerebella. This feature produces a steep posterior face of the cerebellar mass (Fig. 3*B,C*).

Morphometric analysis was used to quantitatively evaluate differences in the mutants. In young adults, there was a reduction in the area of the granule cell layer in $Zic1^{+/-}$ (Fig. 5), consistent with a previous study (Aruga et al., 1998). In the $Zic2^{+/kd}$, there was a slight reduction of the granule cell layer area of the hemisphere. A slight reduction in the hemisphere was also observed in 1-year-old $Zic2^{+/kd}$ cerebellum (data not shown). In contrast to the cerebella of single mutants, the $Zic1^{+/-}Zic2^{+/kd}$ cerebella showed a marked reduction in the area of both granule cell layer and molecular layer. The reduction was more than that of single mutants. The area (mass) reduction reflected a decrease

in the number of granule cells because the cell density of the granule cell layer was not changed ($Zic1^{+/+}Zic2^{+/+}$, $4.4 \times 10^5 \pm 2.5 \times 10^4$ (cells/mm^2); $Zic1^{+/-}Zic2^{+/+}$, $4.3 \times 10^5 \pm 4.9 \times 10^4$; $Zic1^{+/+}Zic2^{+/kd}$, $4.3 \times 10^5 \pm 5.0 \times 10^4$; $Zic1^{+/-}Zic2^{+/kd}$, $4.2 \times 10^5 \pm 5.0 \times 10^4$).

In contrast to the folial pattern abnormalities, laminar organization of the cerebellar cortex is not disturbed, and the Purkinje and granule cell markers were expressed properly (data not shown), indicating that lineage-specific differentiation occurs normally in $Zic1^{+/-}Zic2^{+/kd}$ mice.

Abnormalities in the developing cerebella

To understand how these malformations occurred, we examined the developing cerebella. At E18, the folial pattern of the $Zic1^{+/-}Zic2^{+/kd}$ was distinct from the wild type (Fig. 6*C,D*). The primary fissure was located anteriorly in the cerebellum. Correspondingly, the immature Purkinje cells, which were aligned in a defined pattern along the AP axis, were shifted anteriorly, resulting in the shorter anterior segment (Fig. 6*E,F*).
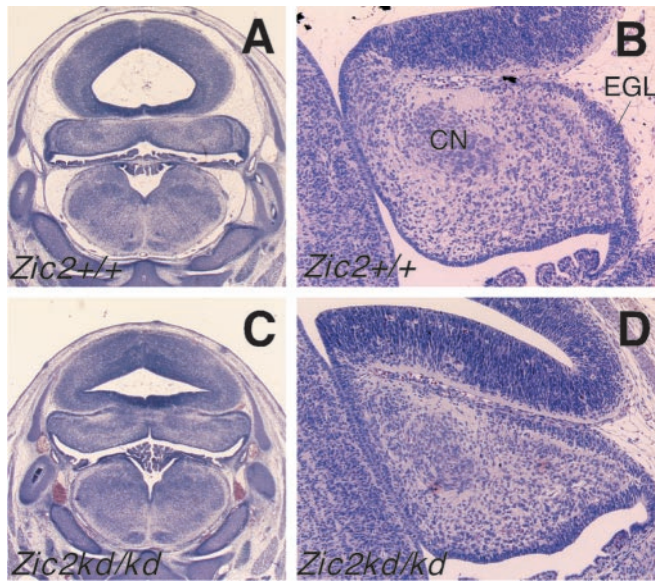
Figure 2. Cerebellar phenotype in *Zic2* knock-down mice. Coronal (*A, C*) and sagittal (*B, D*) hematoxylin and eosin-stained sections were prepared from E16 wild-type (*Zic2*$^{+/+}$) (*A, B*) and *Zic2*$^{kd/kd}$ (*C, D*) embryos. The distorted shape suggests oppression, which is probably caused by disturbed CSF circulation. It is difficult to judge whether *Zic2* has a primary role in the cerebellar development, from *Zic2*$^{kd/kd}$ phenotypes. *CN*, Cerebellar nuclei forming cells; *EGL*, external germinal cell layer.

These features are similar to those of *Zic1*$^{-/-}$ mice (Fig. 6*A,B*). The folial pattern abnormality could be traced back to E17.5 when the position of the initial primary fissure was located more anteriorly in the *Zic1*$^{+/-}$*Zic2*$^{+/kd}$ (data not shown). Ephrin receptors are differentially expressed along the AP axis in the cerebellar primordium (Rogers et al., 1999). The EphA3 receptor, which is usually expressed in the lobule VI region, was detected more anteriorly at E16.5 (Fig. 6*G,H*). We therefore concluded that the cerebellar patterning along AP axis had been differentially established at this point.

We also examined the patterning abnormality along the medial to lateral axis. At E18, a comparison of coronal sections revealed poorly formed foliations in the hemisphere of the *Zic1*$^{+/-}$*Zic2*$^{+/kd}$ cerebella without obvious alteration in medial to lateral extension of the cerebellar mass or the location of the cerebellar nuclei (Fig. 6*I,J*). *En2* is expressed in three parasagittal stripes in horizontal sections of the cerebellar primordium (Millen et al., 1995). This three-striped pattern was also evident in the *Zic1*$^{+/-}$*Zic2*$^{+/kd}$ cerebellum (Fig. 6*K,L*), suggesting that the medial to lateral pattern was not grossly affected in the cerebellar primordium. Taken together, these findings indicate a definite patterning abnormality along the AP axis in the *Zic1*$^{+/-}$*Zic2*$^{+/kd}$ cerebellum.

The reduced proliferation in the EGL underlies the *Zic1*$^{+/-}$*Zic2*$^{+/kd}$ cerebellar abnormality

Our previous study on *Zic1*$^{-/-}$ mice showed that proliferating granule cell precursor levels were decreased in the EGL (Aruga et al., 1998). To examine whether a similar change occurs in *Zic1*$^{+/-}$*Zic2*$^{+/kd}$, numbers of mitotic cells were compared. At E16, mitotic cells were decreased in the EGL, but not in the intermediate zone or the ventricular zone (Fig. 7*A*). At E17.5, the greatest difference was seen in the EGL anterior to the primary fissure (Fig. 7*B*). In contrast to the anterior EGL segment, the reductions in the posterior segment were slight. Mitotic cell
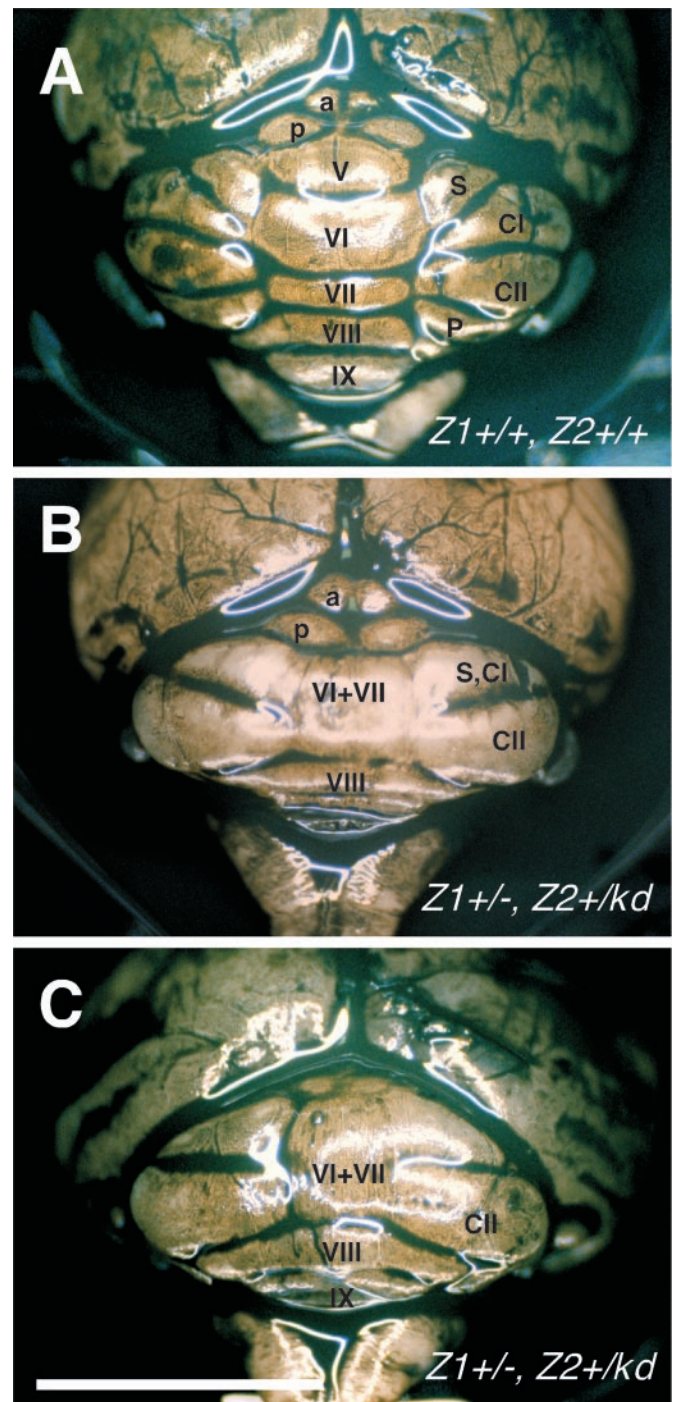

Figure 3. Macroscopic observation of the *Zic1*$^{+/-}$*Zic2*$^{+/kd}$ cerebella. Cerebella from wild-type (*Zic1*$^{+/+}$*Zic2*$^{+/+}$) (*A*) and *Zic1*$^{+/-}$*Zic2*$^{+/kd}$ (*B, C*) at P17 are seen from dorsoposterior (*A, B*) or posterior (*C*) direction. Folial patterns are markedly altered in the *Zic1*$^{+/-}$*Zic2*$^{+/kd}$, different from that of *Zic1*$^{-/-}$. Vermis lobules are indicated by *V–IX*. *a*, Anterior colliculus; *p*, posterior colliculus; *CI*, CrusI lobule; *CII*, CrusII lobule; *S*, simplex lobule; *P*, paramedian lobule. Scale bar, 5 mm.

number per a unit length (1 mm) was significantly decreased only in the E16 EGL (Fig. 7*C*), suggesting that the reduction of the total mitotic cell numbers at E17 reflects an impaired cell proliferation at the preceding stage. In contrast to the abnormality in cell proliferation, there was no change in cell death frequency (data not shown). These results indicate that a reduction in
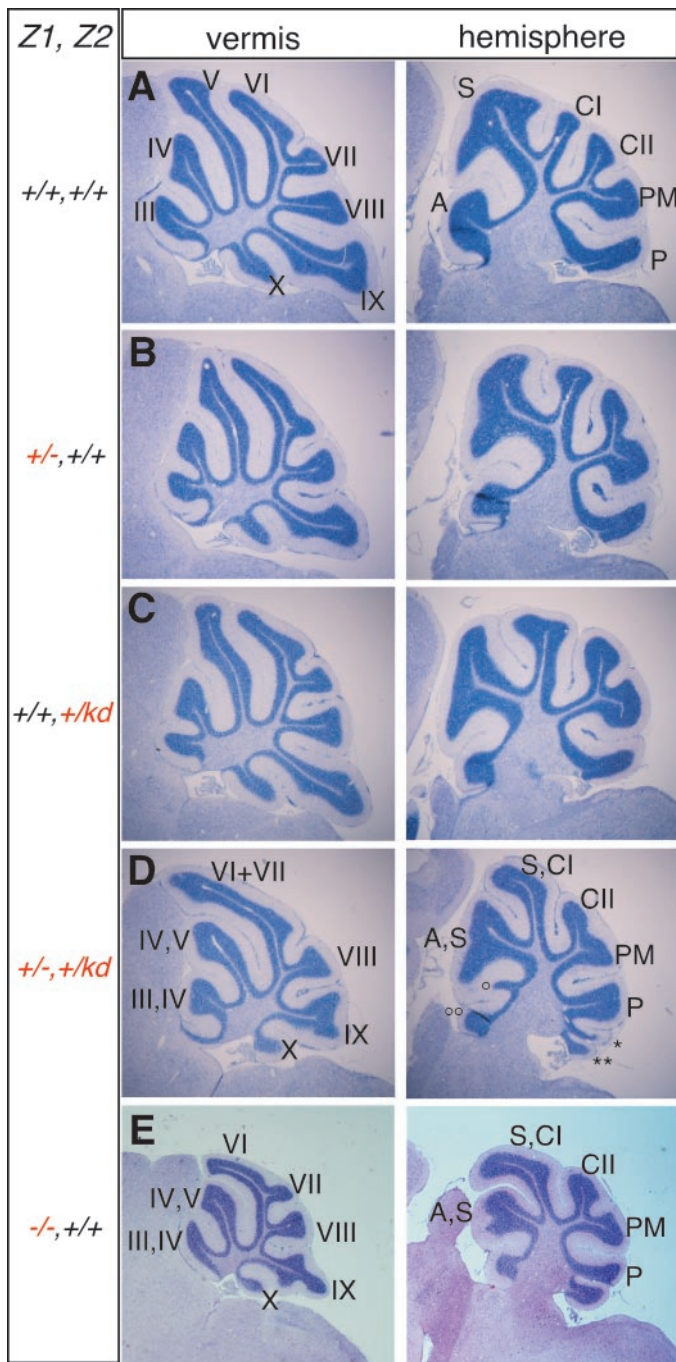
Figure 4. Comparison of the cerebellar folial patterns in sections. Sagittal sections through cerebellar vermis (*left*) and hemisphere (*right*) from $Zic1^{+/+}Zic2^{+/+}$ (*A*), $Zic1^{+/-}Zic2^{+/+}$ (*B*), $Zic1^{+/+}Zic2^{+/kd}$ (*C*), $Zic1^{+/-}Zic2^{+/kd}$ (*D*), and $Zic1^{-/-}Zic2^{+/+}$ (*E*), at P16 (*A–D*) or 3 weeks (*E*) mice. Vermis lobules are indicated by *III–X*. *A*, Anterior lobe; *CI*, CrusI lobule; *CII*, CrusII lobule; *S*, simplex lobule; *PM*, paramedian lobule; *P*, pyramidis. *Asterisks* indicate dorsal (*) and ventral (**) paraflocculus lobules. *Circles* indicate abnormally located lobules, which are not assigned at this point.

proliferating granule cell precursors is a notable feature in the $Zic1^{+/-}Zic2^{+/kd}$ cerebellum.

Progression of neuronal cell differentiation is deregulated in the $Zic1^{-/-}$ and $Zic1^{+/-}Zic2^{+/kd}$ cerebella

Recent studies revealed several genes controlling cerebellar development. We tested their expression in the $Zic1^{-/-}$ and
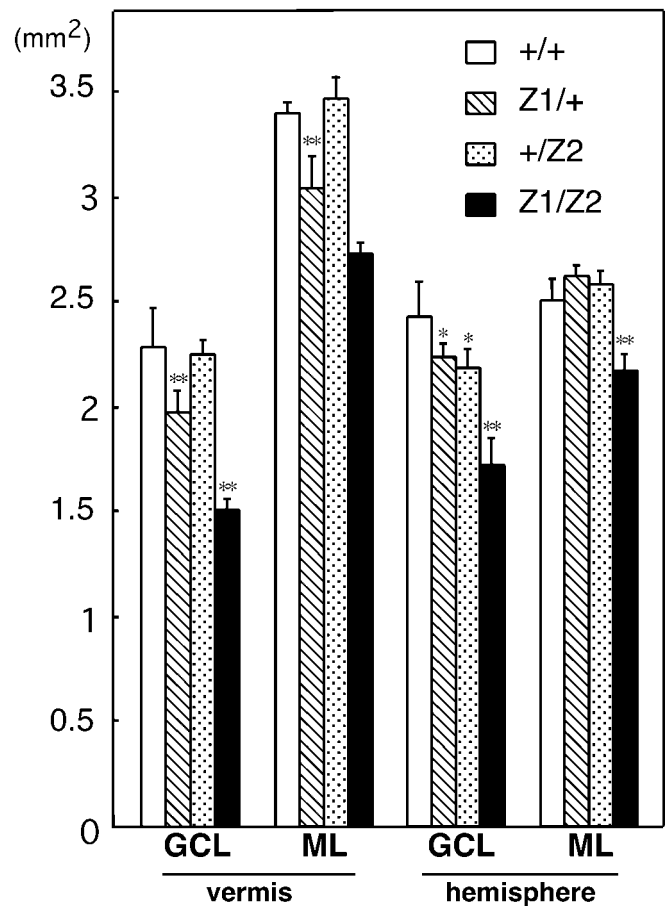

Figure 5. Morphometric analyses of the mutant cerebella. The areas of the granular cell layer (*GCL*) and the molecular layer (*ML*) in midsagittal (*vermis*) and parasagittal sections through hemisphere (*hemisphere*) were measured. The cerebella were derived from P16 single litter. The areas are indicated in square millimeters. The error bars indicate SD. *White bar*, $Zic1^{+/+}Zic2^{+/+}$ (+/+); *black bar*, $Zic1^{+/-}Zic2^{+/kd}$ (Z1/Z2); *hatched bar*, $Zic1^{+/-}Zic2^{+/+}$ (Z1/+); *stippled bar*, $Zic1^{+/+}Zic2^{+/kd}$ (+/Z2); *p < 0.05; **p < 0.01.

$Zic1^{+/-}Zic2^{+/kd}$ mice to evaluate their relationship with Zic proteins. Transcript levels of *cyclin D1*, *cyclin D2*, *p27*, and *Wnt7a* were quantitated in the cerebella of E17.5 $Zic1^{+/-}Zic2^{+/kd}$, $Zic1^{-/-}$ and their littermate wild-type controls (Fig. 8). D-cyclins are thought to drive cell cycle progression by regulating the phosphorylation of cellular substrates by the cyclin-dependent kinases Cdk4 and Cdk6 (Sherr and Roberts, 1999). *Cyclin D1* levels were clearly decreased both in the $Zic1^{+/-}Zic2^{+/kd}$ and $Zic1^{-/-}$ cerebella, whereas the amount of *cyclin D2* was not significantly changed. On the other hand, the Cdk inhibitor *p27*, which stops proliferation of granule cell precursors (Miyazawa et al., 2000), was increased in $Zic1^{-/-}$ and slightly increased in $Zic1^{+/-}Zic2^{+/kd}$. In addition, expression of *Wnt7a*, which is usually expressed in the granule neurons postnatally (Lucas and Salinas, 1997), was prematurely enhanced both in $Zic1^{+/-}Zic2^{+/kd}$ and $Zic1^{-/-}$.

To further examine whether neuronal differentiation is affected, we performed immunohistochemical staining on the E15 cerebella. We detected a significant change in the distribution of the βIII tubulin protein, which is a marker of the differentiated neuron. In the $Zic1^{-/-}$ cerebellum, the region of clustered cerebellar nuclei forming cells where both the *Zic1* and *Zic2* tran-
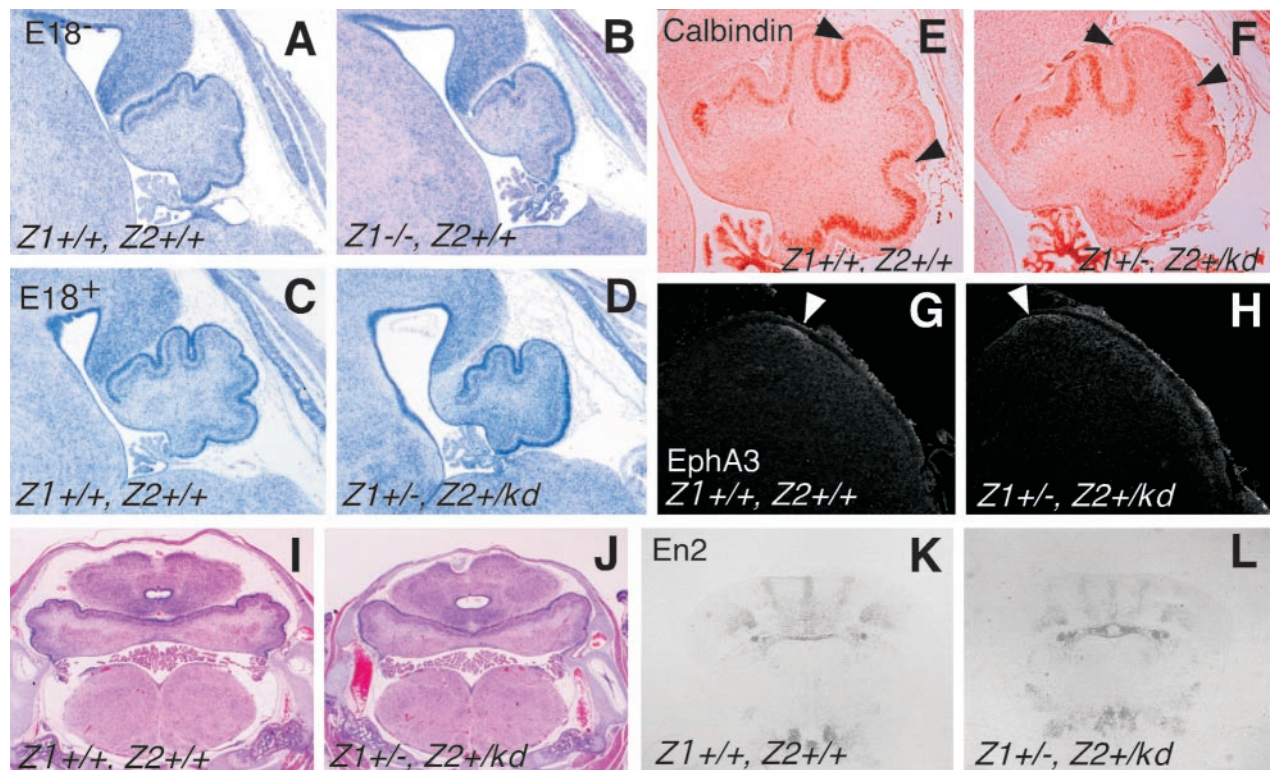
Figure 6. Anterior to posterior patterning abnormality found in the $Zic1^{+/-}Zic2^{+/kd}$ cerebella. Sagittal sections from E18 (*A–F*) and E16 (*G, H*) cerebella of $Zic1^{+/+}Zic2^{+/+}$ (*A, C, E, G*), $Zic1^{-/-}Zic2^{+/+}$ (*B*), and $Zic1^{+/-}Zic2^{+/kd}$ (*D, F, H*). *A, C, E,* and *G* are the littermates of *B, D, F,* and *H,* respectively. *A–D,* Hematoxylin and eosin staining; *E, F,* immunohistochemical staining using anti-calbindin antibody (immature Purkinje cells). *Arrowheads* indicate the corresponding posterior and anterior boundaries of the clusters of Purkinje cells. *G, H,* Anti-EphA3 antibody staining, which stains a transversal zone corresponding to prospective lobule VII. *Arrowheads* indicate the strongly stained zone in each panel. *I, J,* Coronal sections of E18 $Zic1^{+/+}Zic2^{+/+}$ (*I*) and $Zic1^{+/-}Zic2^{+/kd}$ (*J*) embryos. *K, L, En2* expression in the E17 horizontal section of $Zic1^{+/+}Zic2^{+/+}$ (*K*) and $Zic1^{+/-}Zic2^{+/kd}$ (*L*) are shown by *in situ* hybridization. Note that the anterior region is reduced, as indicated by the folial and the marker expression patterns, whereas there are no apparent abnormalities in the medial to lateral patterning.

scripts were detected (Fig. 1*K,O*) was more strongly stained with the anti-βIII tubulin antibody than the wild-type control (Fig. 9*A,B*). Corresponding areas contained more strongly p16-immunopositive cells (Fig. 9*C,D*). The $Zic1^{+/-}Zic2^{+/kd}$ cerebella showed a slightly enhanced distribution of βIII tubulin protein in the corresponding region (data not shown). These results indicate that premature neuronal differentiation occurs in both $Zic1^{+/-}Zic2^{+/kd}$ and $Zic1^{-/-}$ cerebella at this stage.

DISCUSSION

Functional cooperation between *Zic1* and *Zic2* in cerebellar development

This study investigated the involvement of *Zic2* in cerebellar development by generating $Zic1^{+/-}Zic2^{+/kd}$ mutant mice. The $Zic1^{+/-}$ and $Zic2^{+/kd}$ cerebella were almost indistinguishable from wild type, although a subtle reduction of the size was observed in both the $Zic1^{+/-}$ and $Zic2^{+/kd}$. In contrast, the $Zic1^{+/-}Zic2^{+/kd}$ cerebellum was abnormal and distinct from wild type. This is the first evidence for the cooperative role of the Zic family of genes in vertebrate development. Besides the cerebellar abnormality, $Zic1^{+/-}Zic2^{+/kd}$ mice also showed changes in the septum, which was not affected either in $Zic1^{+/-}$ or $Zic2^{+/kd}$ (J. Aruga, unpublished observation). These findings are consistent with the idea that Zic1 and Zic2 proteins have essentially similar functions. This idea is also supported by a recent study revealing that both Zic1 and Zic2 have similar DNA-binding properties

and that both activate reporter genes in cultured cells (Mizugishi et al., 2001).

How can we explain the phenotypic difference between $Zic1^{-/-}$ and $Zic2^{kd/kd}$ mice? The difference may be attributed to the difference in the spatiotemporal expression patterns. At a primitive streak stage, *Zic2* expression is strong in the forebrain region while *Zic1* expression occurs later in the neuroectoderm and is enhanced in the hindbrain and the spinal cord (Nagai et al., 1997). This may explain the absence of apparent forebrain abnormality in the *Zic1* mutant. It remains inconclusive as to whether the cerebellar phenotype of the $Zic2^{kd/kd}$ mice reflects the lack of intrinsic *Zic2* function in the cerebellum. Because the malformation of the posterior neuropore and forebrain is obvious as early as E9.5 and E10.5, respectively, cerebellar development may be secondarily affected by the preceding malformation.

Although *Zic1* and *Zic2* appear to have largely redundant functions, there remains the possibility that specific *Zic1/Zic2* interactions are required for cerebellar development. This could explain why the folial pattern in the trans-heterozygote is not identical to that found in $Zic1^{-/-}$. A "swapping" experiment (Hanks et al., 1995) is required to further investigate the functional equivalency of both proteins.

The role of *Zic1* and *Zic2* in cerebellar development

We suggest that Zic1 and Zic2 proteins may have following roles in cerebellar development. One is the regulation of
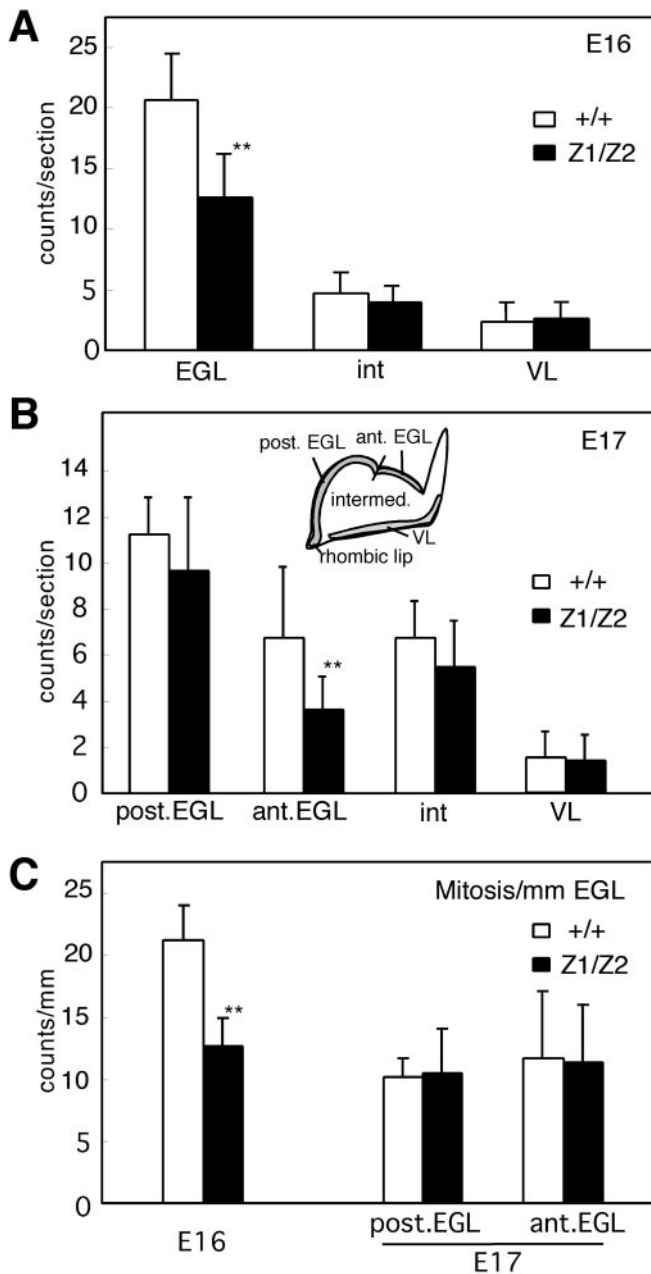
Figure 7. Proliferating cell numbers in the *Zic1/Zic2* cerebellum. Cells stained with anti-phospho-histone H3 antibodies (mitotic cells) were counted in the indicated regions of the E16 (*A*) and E17 (*B*) cerebellar sagittal sections. The ordinate indicates the mean number of the labeled cells per section. In *C*, mean numbers of the labeled cells in 1 mm of the EGL are indicated. The error bars indicate SD. *ant EGL*, Anterior EGL; *post EGL*, posterior EGL; *VL*, ventricular layer; *int* (*intermed*), intermediate zone that includes the area in the cerebellar primorium except EGL and VL; +/+, *Zic1$^{+/+}$Zic2$^{+/+}$*; Z1/Z2, *Zic1$^{+/-}$Zic2$^{+/kd}$*; **$p < 0.01$

Figure 8. Genes controlling cerebellar development are deregulated in the *Zic1$^{-/-}$* and *Zic1$^{+/-}$Zic2$^{+/kd}$* cerebella. RT-PCR analysis was performed on cDNAs prepared from cerebella of E17.5 *Zic1$^{-/-}$* and *Zic1$^{+/-}$Zic2$^{+/kd}$* and their littermate wild-type controls. *G3PDH* is a ubiquitously expressed gene. In the absence of reverse transcriptase [*G3PDH* (-RT)], no bands are detected, ensuring the absence of DNA. Amounts of *cyclin D1*, *cyclin D2*, *p27*, and *Wnt7a* transcripts were compared.

granule cell expansion by Zic proteins. Our previous study showed that decrease in granule cell number is the most significant change in the *Zic1$^{-/-}$* cerebella. This was partly explained by the reduction in cell proliferation of the granule cell precursors. In the *Zic1$^{+/-}$Zic2$^{+/kd}$* cerebella, the level of proliferating cells was significantly reduced at the beginning of phenotypic expression in the EGL. Because both *Zic1* and *Zic2* are expressed in the granule cell precursors in a similar man-
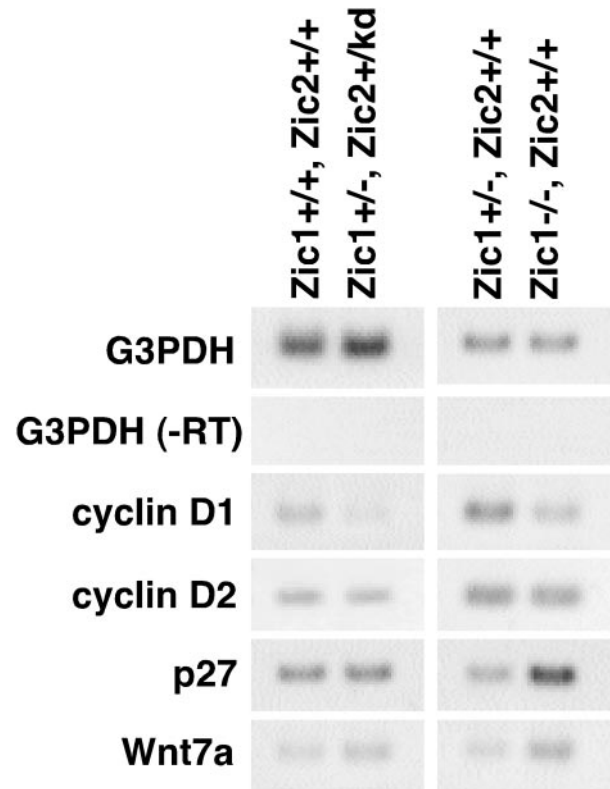
ner, it is likely that *Zic2* controls granule cell proliferation in a similar manner to *Zic1*.

The stimulation of granule cell proliferation by *Zic1* and *Zic2* proteins may be regulated via the expression of cell cycle regulatory genes. *cyclin D1*, which was decreased in the mutant mouse cerebella, is known to drive cell proliferation in multiple tissues (Fantl et al., 1995; Sicinski et al., 1995). In addition, another member of the D-cyclin family, *cyclin D2*, which is predominantly expressed in the postnatal EGL (Ross et al., 1996), was shown to control cerebellar histogenesis (Huard et al., 1999). Although cerebellar abnormalities have not been reported in cyclin D1-deficient mice (Fantl et al., 1995; Sicinski et al., 1995), it is possible that *cyclin D1* normally contributes to the control of granule cell proliferation and that its function is compensated for by other related molecules. The enhanced expression of *p27* may be acting synergistically in the reduction of cell proliferation in the granule cell precursors, because deletion of the *p27* gene restores normal development in cyclin D1-deficient mice (Geng et al., 2001).

In addition to their expression in granule cells and their precursors, both *Zic1* and *Zic2* are also expressed in the midline and anterior part of the vermal region of the cerebellar primordia at E16 and E18. This region contains clusters of cerebellar nuclei forming cells. The progression of neuronal differentiation in this region was affected in the *Zic1$^{+/-}$Zic2$^{+/kd}$* and *Zic1$^{-/-}$* cerebella. In addition, there was a difference in the expression pattern
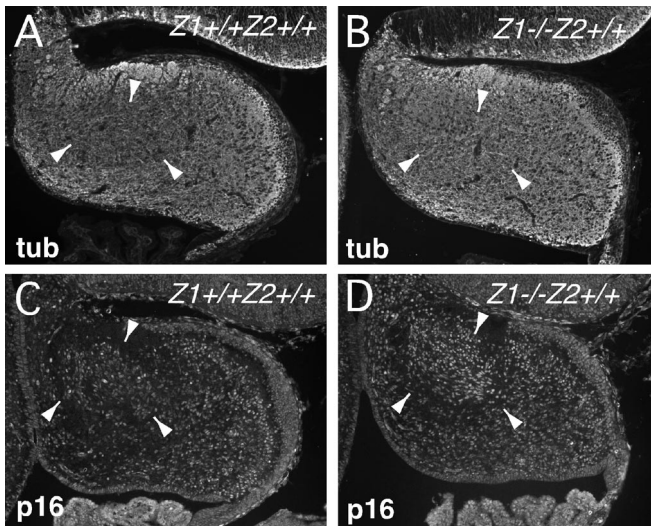
Figure 9. Premature neuronal differentiation occurs in the *Zic1*$^{-/-}$ cerebella. Immunohistochemical staining showing localization of βIII tubulin (*A, B*) and p16 (*C, D*) proteins were examined in the in E16 cerebella of *Zic1*$^{-/-}$. Wild-type littermates (*A, C*) are shown as controls for *B* and *D*, respectively. The area surrounded by the *arrowheads* indicates the corresponding region between the mutants and wild-type controls, which showed significant differences.

between *Zic1* and *Zic2*, which also may participate in generating the difference in the folial pattern between these two mutants.

We recently observed an inhibitory effect of mis-expressed *Zic1* in the neuronal differentiation in chick spinal cord (J. Aruga, T. Tohmonda, S. Homma, and K. Mikoshiba, unpublished observations). In addition, Brewster et al. (1998) showed that neuronal differentiation, as indicated by N-tubulin expression, is inhibited by *Xenopus Zic2* expression. These facts suggest that the Zic family of proteins may play a general role in the inhibition of neuronal differentiation, via their effect on the expression of regulatory cell cycle genes. It is interesting that the Zic proteins are able to promote the differentiation of neuroectoderm from ectoderm in the *Xenopus* embryo (Nakata et al., 1997, 1998), while at the same time inhibit neuronal differentiation. Zic proteins are also expected to have another role in the adult granule neuron, whereas all Zic genes are abundantly expressed.

Although this study showed that *cyclin D1, p27,* and *Wnt7a* are possible targets of the Zic proteins as transcriptional regulators, it is not clear how the Zic proteins act in the regulatory process. A comprehensive analysis of the downstream target genes and the assessment of possible relationships with other regulatory molecules are necessary for further understanding. Recent studies have indicated a functional interaction between Zic proteins and Gli proteins, which share a highly conserved zinc finger domain (Aruga et al., 1996, 1999; Brewster et al., 1998; Koyabu et al., 2001; Mizugishi et al., 2001). *Gli* genes are also expressed in developing cerebella and mediate Shh signaling which enhances proliferation of granule cell precursors (Wechsler-Reya and Scott, 1999). The role of the Gli proteins in cerebellar development has not yet been shown, and the intriguing question of their relevance to Zic proteins is still to be answered.

REFERENCES

Altman J, Bayer SA (1997) Comparative anatomy of the cerebellum, an evolutionally perspective. In: Development of the cerebellar system, pp 3–20. New York: CRC.

Aruga J, Yokota N, Hashimoto M, Furuichi T, Fukuda M, Mikoshiba K (1994) A novel zinc finger protein, Zic, is involved in neurogenesis, especially in the cell lineage of cerebellar granule cells. J Neurochem 63:1880–1890.

Aruga J, Nagai T, Tokuyama T, Hayashizaki Y, Okazaki Y, Chapman VM, Mikoshiba K (1996) The mouse Zic gene family: homologues of Drosophila pair-rule gene odd-paired. J Biol Chem 271:1043–1047.

Aruga J, Minowa O, Yaginuma H, Kuno J, Nagai T, Noda T, Mikoshiba K (1998) Mouse Zic1 is involved in cerebellar development. J Neurosci 18:284–293.

Aruga J, Mizugishi K, Koseki H, Imai K, Balling R, Noda T, Mikoshiba K (1999) Zic1 regulates the patterning of vertebral arches in cooperation with Gli3. Mech Dev 89:141–150.

Brewster R, Lee J, Ruiz I, Altaba A (1998) Gli/Zic factors pattern the neural plate by defining domains of cell differentiation. Nature 393:579–583.

Fantl V, Stamp G, Andrews A, Rosewell I, Dickson C (1995) Mice lacking cyclin D1 are small and show defects in eye and mammary gland development. Genes Dev 9:2364–2372.

Geng Y, Yu Q, Sicinska E, Das M, Bronson RT, Sicinski P (2001) Deletion of the p27/Kip1 gene restores normal development in cyclin D1-deficient mice. Proc Natl Acad Sci USA 98:194–199.

Goldowitz D, Hamre K (1998) The cells and molecules that make a cerebellum. Trends Neurosci 21:375–382.

Hanks M, Wurst W, Anson-Cartwright L, Auerbach AB, Joyner AL (1995) Rescue of the En-1 mutant phenotype by replacement of En-1 with En-2. Science 269:679–682.

Hatten ME, Alder J, Zimmerman K, Heintz N (1997) Genes involved in cerebellar cell specification and differentiation. Curr Opin Neurobiol 7:40–47.

Herrup K, Kuemerle B (1997) The compartmentalization of the cerebellum. Annu Rev Neurosci 20:61–90.

Huard JM, Forster CC, Carter ML, Sicinski P, Ross ME (1999) Cerebellar histogenesis is disturbed in mice lacking cyclin D2. Development 126:1927–1935.

Koyabu Y, Nakata K, Mizugishi K, Aruga J, Mikoshiba K (2001) Physical and functional interactions between Zic and Gli proteins. J Biol Chem 276:6889–6892.

Lucas FR, Salinas PC (1997) WNT-7a induces axonal remodeling and increases synapsin I levels in cerebellar neurons. Dev Biol 192:31–44.

Millen KJ, Hui C-c, Joyner AL (1995) A role for En-2 and other murine homologues of *Drosophila* segment polarity genes in regulating positional information in the developing cerebellum. Development 121:3935–3945.

Miyazawa K, Himi T, Garcia V, Yamagishi H, Sato S, Ishizaki Y (2000) A role for p27/Kip1 in the control of cerebellar granule cell precursor proliferation. J Neurosci 20:5756–5763.

Mizugishi K, Aruga J, Nakata K, Mikoshiba K (2001) Molecular properties of Zic proteins as transcriptional regulators and their relationship to GLI proteins. J Biol Chem 276:2180–2188.

Nagai T, Aruga J, Takada S, Gunther T, Sporle R, Schughart K, Mikoshiba K (1997) The expression of the mouse Zic1, Zic2 and Zic3 gene suggests an essential role for Zic gene in body pattern formation. Dev Biol 182:299–313.

Nagai T, Aruga J, Minowa O, Sugimoto T, Ohno Y, Noda T, Mikoshiba K (2000) Zic2 regulates the kinetics of neurulation. Proc Natl Acad Sci USA 97:1618–1623.

Nakata K, Nagai T, Aruga J, Mikoshiba K (1997) Xenopus Zic3, a primary regulator both in neural and neural crest development. Proc Natl Acad Sci USA 94:11980–11985.

Nakata K, Nagai T, Aruga J, Mikoshiba K (1998) Xenopus Zic family and its role in neural and neural crest development. Mech Dev 75:43–51.

Rogers JH, Ciossek T, Menzel P, Pasquale EB (1999) Eph receptors and ephrins demarcate cerebellar lobules before and during their formation. Mech Dev 87:119–128.

Ross ME, Carter ML, Lee JH (1996) MN20, a D2 cyclin, is transiently expressed in selected neural populations during embryogenesis. J Neurosci 16:210–219.

Sherr CJ, Roberts JM (1999) CDK inhibitors, positive and negative regulators of G1-phase progression. Genes Dev 13:1501–1512.

Sicinski P, Donaher JL, Parker SB, Li T, Fazeli A, Gardner H, Haslam SZ, Bronson RT, Elledge SJ, Weinberg RA (1995) Cyclin D1 provides a link between development and oncogenesis in the retina and breast. Cell 82:621–630.

Wassef M, Joyner AL (1997) Early mesencephalon/metencephalon patterning and development of the cerebellum. Perspect Dev Neurobiol 5:3–16.

Wechsler-Reya RJ, Scott MP (1999) Control of neuronal precursor proliferation in the cerebellum by sonic hedgehog. Neuron 22:103–114.

Voogd J (1998) Cerebellum and precerebellar nuclei. In: The central nervous system of vertebrates (Nieuwenhuys R, ten Donkelaar HJ, Nicholson C), pp 1724–1753. Berlin: Springer.